Supplemental Information

Anions Mediate Ligand Binding

in _Adineta vaga_ Glutamate Receptor Ion Channels

Suvendu Lomash, Sagar Chittori, Patrick Brown, and Mark L. Mayer

Supplementary Information

Supplementary Figure 1
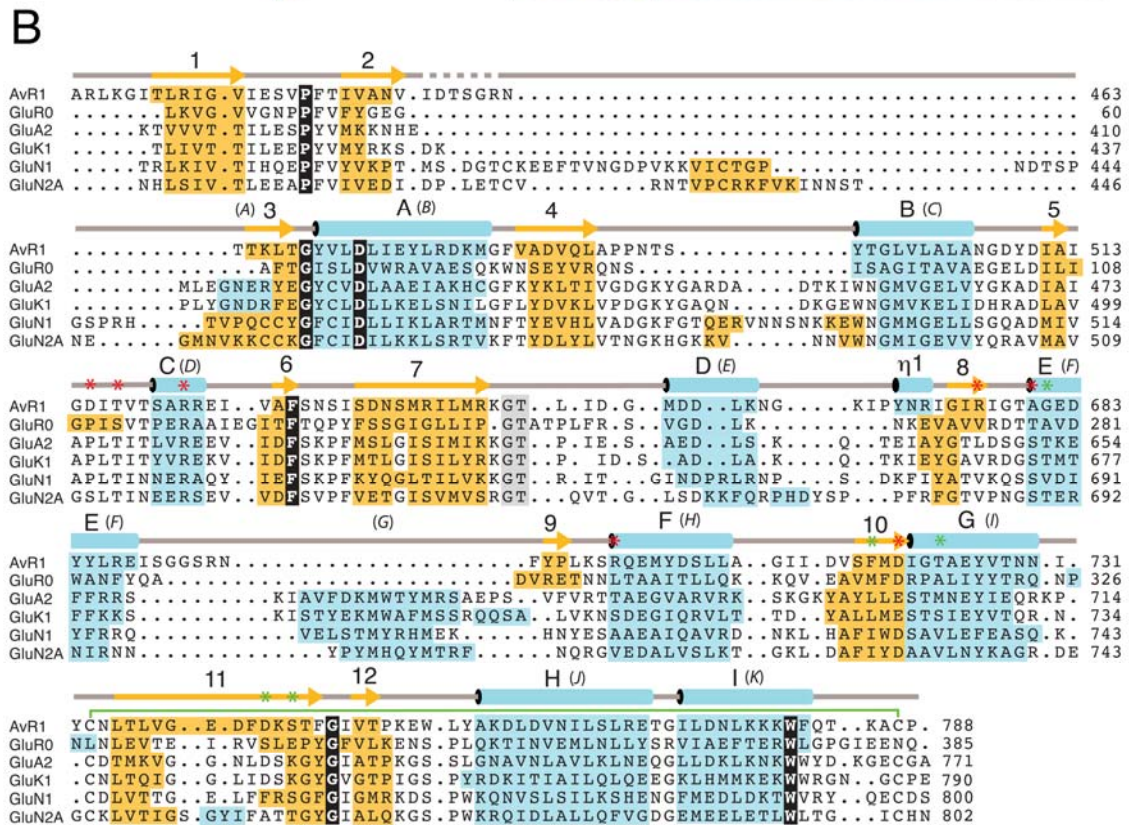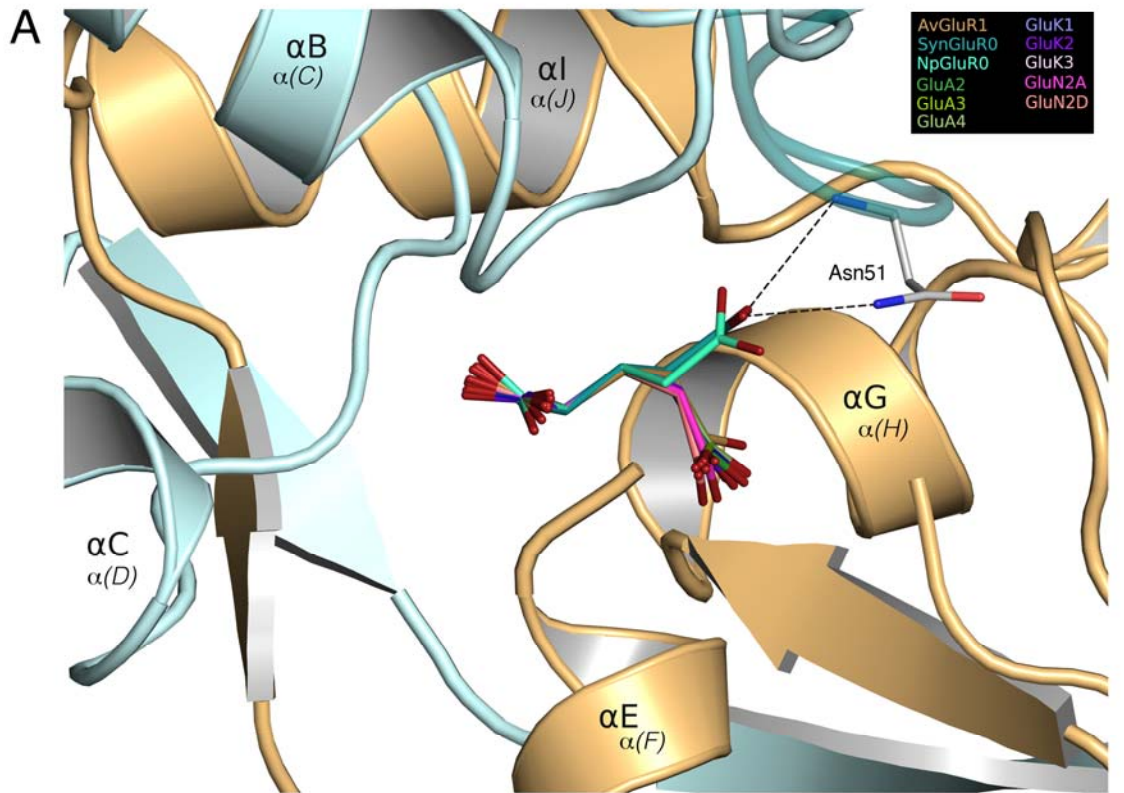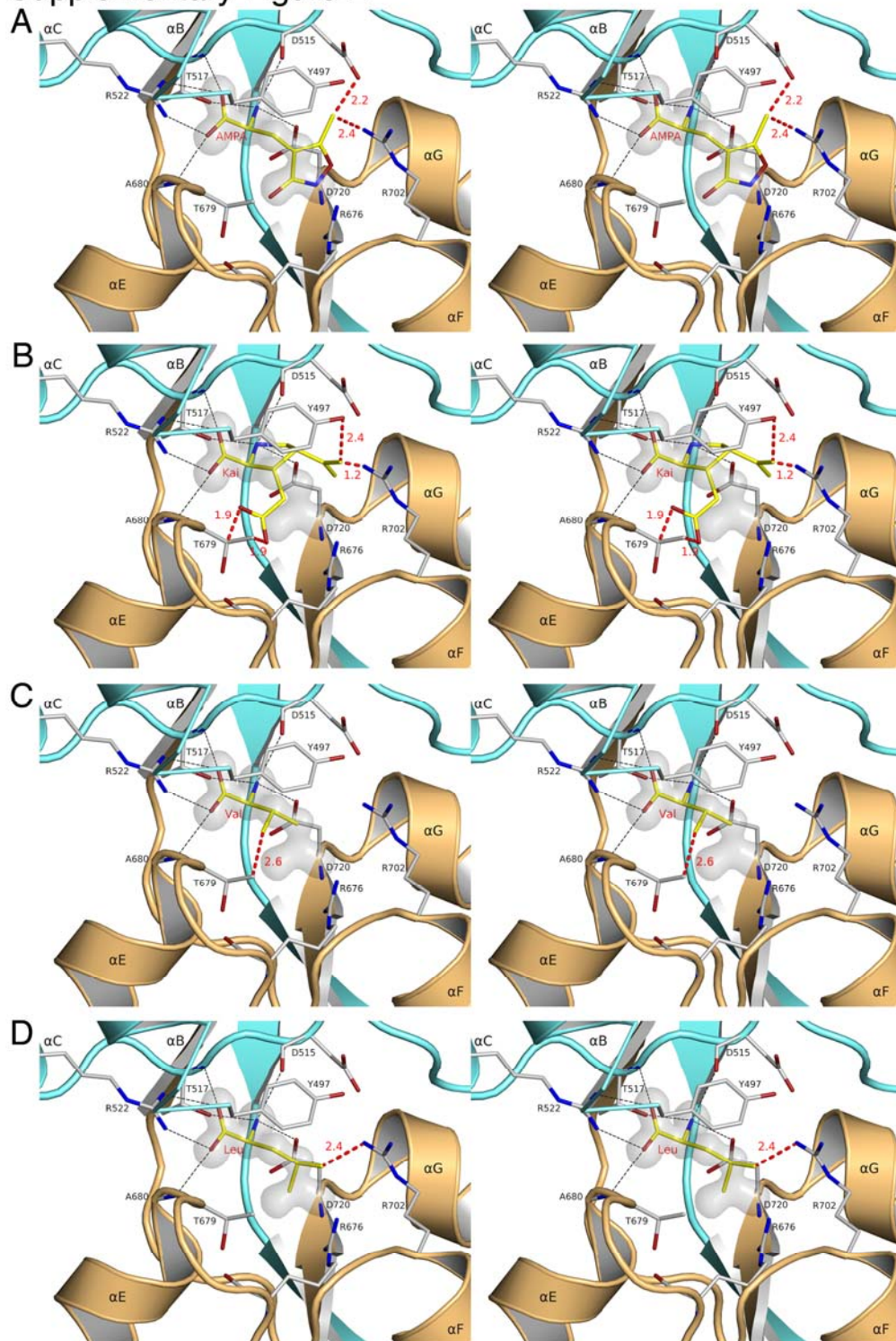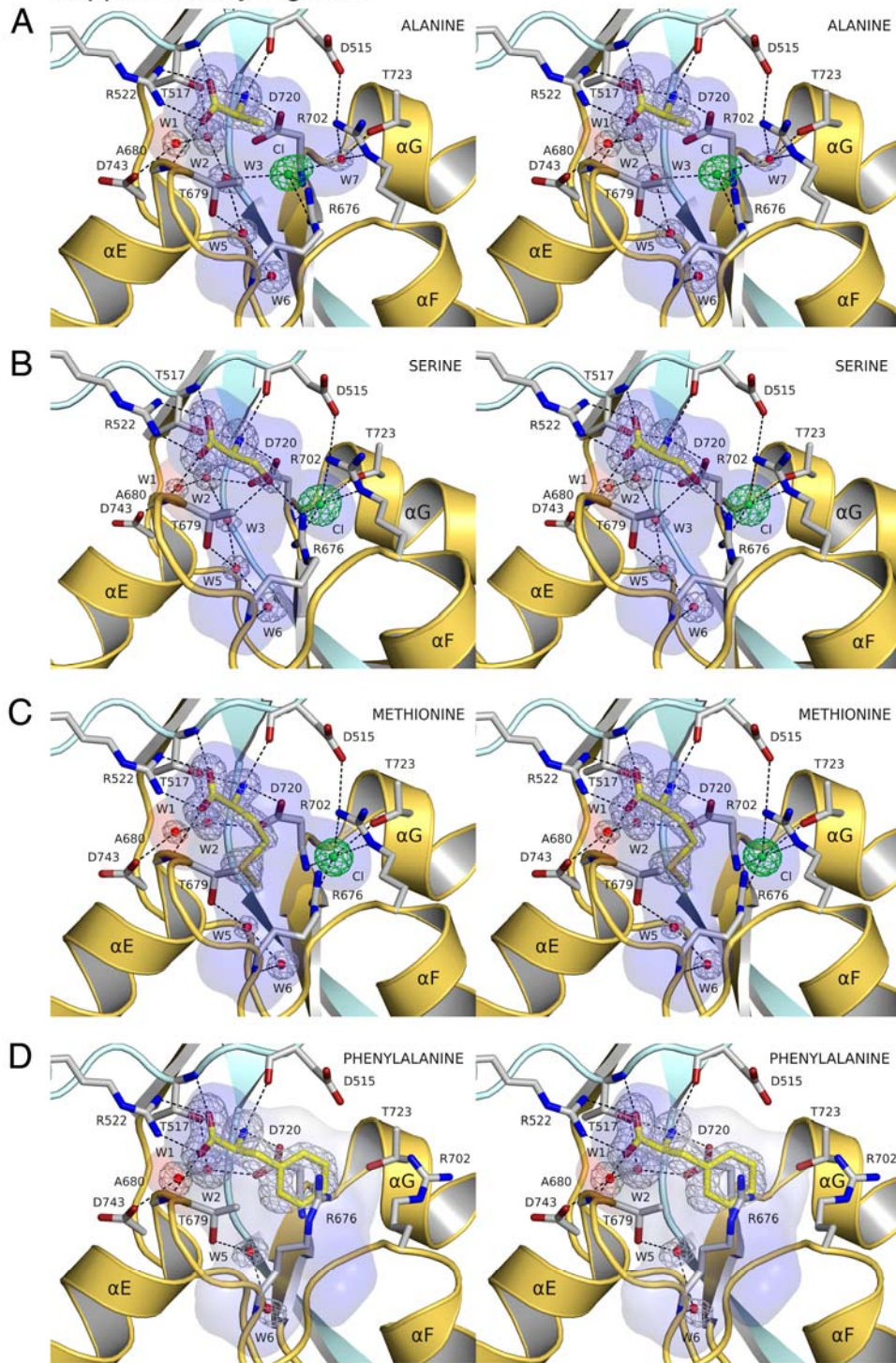
Supplementary Figure 1 related to Figures 3 and 5. **A** Glutamate adopts different conformations in prokaryotic and eukaryotic iGluR LBDs. The ribbon diagram shows the AvGluR1 glutamate complex with the S1 and S2 segments colored cyan and gold respectively; bound glutamate molecules are shown in stick representation for ten iGluR LBD complexes superimposed on AvGluR1 using ligand N, C and Cα coordinates. For 8 eukaryotic iGluRs (α-helices labeled in italics) and for AvGluR1, the γ-carboxyl group projects into domain 2, while for *Synechocystis* and *Nostoc punctiforme* prokaryotic iGluRs glutamate adopts an extended conformation, with the γ-carboxyl group bound by residues in domain 1 as shown for Asn51 and the dark cyan loop from *Synechocystis* GluR0. **B** Structure based sequence alignment for AvGluR1 with representative prokaryotic and eukaryotic iGluRs reveal highly conserved residues widely scattered in linear sequence and not involved in ligand binding (black boxes); cyan and yellow coloring indicates α-helices (and one 3_{10} helix) and β-strands, respectively; α-helices for GluA2 and GluK2 are labeled in italics; gray dots in the AvGluR1 secondary structure schematic indicate six residues in loop 1 for which no main chain electron density was observed; red and green asterisks indicate residues forming direct, or solvent mediated contacts with glutamate, respectively.

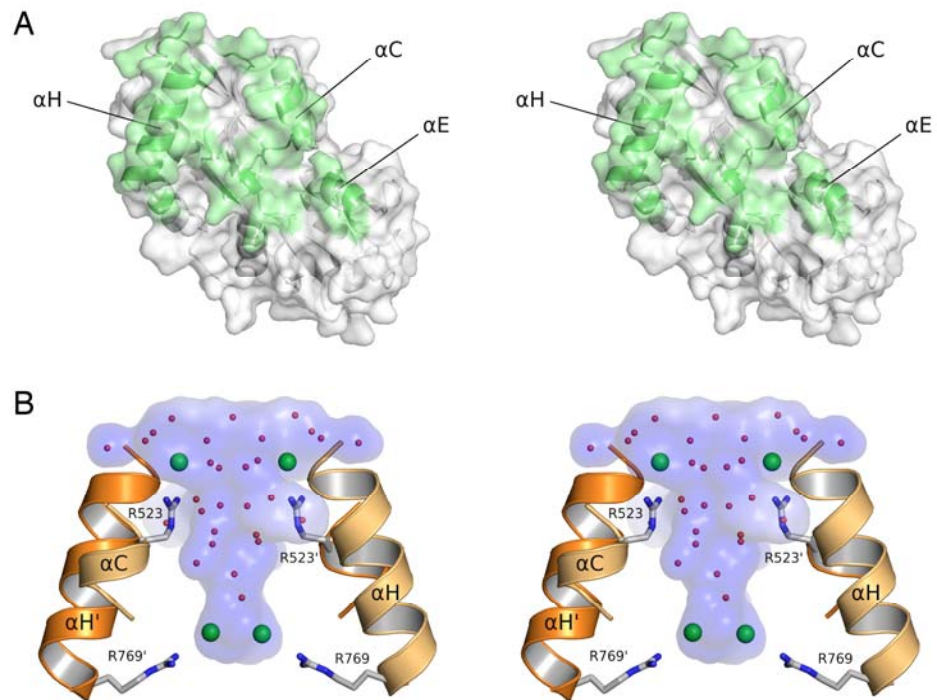**Supplementary Figure 2** related to Figures 3 and 4. Stereoviews of AMPA, kainate valine and leucine docked by least squares superposition of the N, C and Cα atoms on the bound glutamate ligand, with torsion angles adjusted to give the best fit into the omit map for glutamate. Bad van der Waals contacts are indicated by dashed red lines with the contact distance given in Å; favorable H-bonds are drawn as black dashed lines.

Supplementary Figure 3 related to Figure 4. Stereoview of electron density omit map contoured at 5 σ for alanine, serine, methionine and phenylalanine, water molecules and Cl⁻ ions trapped in the AvGluR1 ligand binding cavity.

Supplementary Figure 4

Supplementary Figure 4 related to Figure 7. **A** Stereoview of a single protomer with the buried surface in the dimer assembly colored green; note the tunnel located between α-helices C and H extending towards the base of domain 1. **B** Stereoview rotated by 90° showing α-helices C and H for both subunits in the dimer assembly, with the surface of the tunnel colored by electrostatic potential, showing the location of chloride ions and water molecules.

Ligand	K_d (μM)	
Amino acids		
L-Glu	0.20	± 0.02
L-Asp	0.87	± 0.08
L-Ala	9.27	± 1.24
D-Asp	12.4	± 0.4
L-Met	15.1	± 2.5
L-Ser	24.5	± 1.9
L-Gln	27.0	± 2.5
L-Cys	46.1	± 4.3
L-Asn	81.4	± 13
D-Glu	129	± 10
L-Phe	211	± 45
D-Ser	699	± 60
Gly	966	± 42
L-HCA	5.57	± 0.5
L-AP4	3.82	± 0.8
DL-APA	71.1	± 3.7
Agonists		
Quisqualate	38.7	± 7.9
SYM2081	49.5	± 2.7
AMPA	127	± 16
Kainate	2720	± 486
NMDA	9880	± 1300
Antagonists		
UBP-310	161	± 13
DNQX	250	± 21
DL-AP5	530	± 107

Supplementary Table 1 related to Figure 1. K_d values are mean ± SEM for 3 observations per ligand. Comparing affinities for aspartate, glutamate, α-amino adipic acid (L-AA) and α-amino pimelic acid (DL-APA), where the length of the side chain progressively increases by a methylene group, reveals that similar to GluR0, shortening in case of L-Asp, which produces a 4-fold reduction in affinity, is more easily accommodated than lengthening, as evident from the 180-fold decrease in affinity for L-AA and the 360-fold decrease in affinity for DL-APA. However, different from GluR0, AvGluR1 binds AMPA while affinity for kainate and NMDA is much is much lower.